Analytic solution of the mean elevation of a watershed dominated by fluvial incision and hillslope landslides.

J. Lavé

Analytic solution of the mean elevation of a watershed dominated by fluvial incision and hillslope landslides

J. Lavé

Laboratoire de Géodynamique des Chaînes Alpines, Grenoble, France

Received 19 January 2005; revised 24 March 2005; accepted 3 May 2005; published 9 June 2005.

[1] In active mountainous landscapes dominated by detachment-limited fluvial incision and hillslope landslides, the scaling relations that characterize both river profiles and planimetric organization of the river network can be linked to provide an analytic solution to describe the mean elevation of a watershed. This new analytical approach directly links mountain elevation, precipitation, bedrock erodibility and uplift rate, and yields results that are consistent with those obtained through classic 2-D surface process model. When applied to a growing linear mountain range the approach provides an approximate, but much faster, solution for 2-D or 3-D numerical models of crustal deformation that explicitly include surface processes. **Citation:** Lavé, J. (2005), Analytic solution of the mean elevation of a watershed dominated by fluvial incision and hillslope landslides, *Geophys. Res. Lett.*, *32*, L11403, doi:10.1029/2005GL022482.

1. Introduction

[2] The dominant role of fluvial network in shaping mountainous landscape has been recognized for many years, both as an efficient downcutting agent through fluvial incision and as the major conveyor of eroded material. The channel profile equation of a mountain river can easily be derived from analytic approaches [e.g., *Whipple and Tucker*, 1999]. However, the two-dimensional complex geometry of the fluvial networks has precluded so far a simple analytic description of the mean elevation or the topographic profile of mountain ranges. Several statistical approaches, based on databases of erosional fluxes exported from orogens, have tried to link erosion with average or maximum elevation of mountain ranges or with their climatic setting [e.g., *Pinet and Souriau*, 1988], but have failed to converge toward a consistent model and to incorporate physically based principles. In the absence of a simple analytic description of the physical erosion acting in mountainous landscape, most of the numerical studies focusing on coupling and feedbacks between tectonics, erosion and climate, have generally used simple erosion laws that neglect the complexity arising from the dendritic geometry of fluvial networks. The erosion law chosen when modelling an active orogen can, however, significantly influence the average topographic elevation, and consequently the mechanical coupling between erosion and tectonics [*Godard et al.*, 2004].

[3] Here, we propose an analytic solution, accounting for river network geometry, to compute the mean elevation of a watershed dominated by detachment-limited fluvial incision and hillslope landsliding under constant, uniform uplift rate. An approximated 1-D approach, derived from the analytic solution, is also proposed to compute the temporal evolution and steady state geometry of a growing linear range. The consistency of the analytic solution and 1-D model results is tested by comparing with the results obtained from a classic, but much more time-costly, 2-D surface process model (SPM).

2. Detachment-Limited Fluvial Incision, River Profiles, and Relief

[4] Although several different functional forms have been proposed to model fluvial incision, we adopt a simple detachment-limited relation that has provided satisfactory first-order results across the Subhimalaya [*Lavé and Avouac*, 2001]. This relation states that bedrock incision rate (i) of a river can be expressed as a power function of the fluvial shear stress or the unit stream power, or more generally as a generic function:

$$i = k\left(A^{\gamma}\left(\overline{P} - P_0\right)^{\beta} S^{\alpha} - \varepsilon_0\right) \tag{1}$$

with A the drainage area, S the channel slope, k a dimensional "erodibility" coefficient, ε_0 a minimum treshold for incipient erosion, $\overline{P} = \int_A P(\vec{x})d\vec{x}$ the spatially averaged precipitation over the drainage area, P_0 a runoff threshold, and α, β, γ three positive exponents (see also symbols notation in Text S1 in the auxiliary material[1]). The longest stream (x_l) in a fluvial network generally follows Hack's law: $x_l = k_x A^{\delta}$, with k_x a dimensional coefficient and δ a positive exponent ranging from 0.5 to 1. From the above equations, temporal evolution of a channel elevation (h_r) can be synthesized by:

$$\begin{aligned}\frac{\partial h_r}{\partial t} &= u - i = u - k\left(A^{\gamma}\left(\overline{P} - P_0\right)^{\beta} S^{\alpha} - \varepsilon_0\right) \\ &= u - k\left(k_x^{-\gamma/\delta} x_l^{\gamma/\delta}\left(\overline{P} - P_0\right)^{\beta} S^{\alpha} - \varepsilon_0\right),\end{aligned} \tag{2}$$

with u the rock uplift rate.

[5] At steady state ($i = u$), the channel slope is given by:

$$S = \left|\frac{\partial h_r}{\partial x_l}\right| = \left(\frac{u}{k}(x_l) + \varepsilon_0\right)^{1/\alpha}\left(\overline{P}_{(x_l)} - P_0\right)^{-\beta/\alpha} A^{-\gamma/\alpha}. \tag{3}$$

0094-8276/05/2005GL022482

[1] Auxiliary material is available at ftp://ftp.agu.org/apend/gl/2005GL022482.

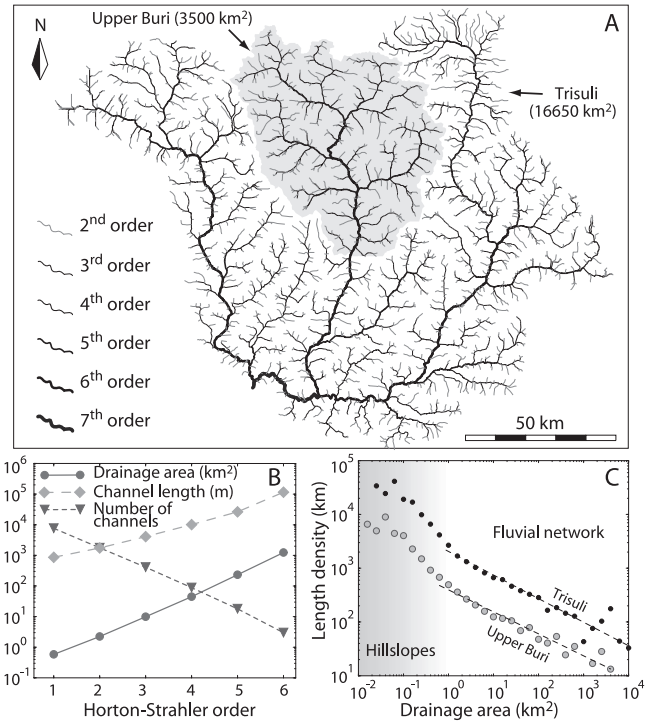

Figure 1. (a) Trisuli fluvial network with Horton-Strahler orders, computed for a minimum source area of A_1 = 0.5 km^2, and automatically extracted from a 90m DEM of central Nepal. (b) Scaling laws characterizing this Horton's ordering ($R_N \cong 4.7$, $R_L \cong 2.35$, $R_A \cong 4.7$ and $\frac{Ln(R_L)-Ln(R_N)}{Ln(R_A)} = -0.44$). (c) River network length density function, displayed as a histogram employing logarithmic bin widths ($\log_{10} w = 1/5$), for the Trisuli watershed (black dots) and for the upper portion (shaded area in Figure 1a) of the Buri watershed (gray circles). In the fluvial network domain (A > 0.5–1 km^2), the slope exponent of the distribution is (1-ω) = -0.44 ± 0.03. See color version of this figure in the HTML.

In the case of uniform uplift, precipitation and lithology, the equilibrium river profile becomes:

$$h_r(x_l) \cong h_0 - \frac{k_x^{+\gamma/\alpha\delta}}{(1-\gamma/\alpha\delta)} U_*^{1/\alpha}\left(x_l^{1-\gamma/\alpha\delta} - x_0^{1-\gamma/\alpha\delta}\right) \quad \text{if } \gamma/\alpha\delta \neq 1 \tag{4a}$$

and

$$h_r(x_l) \cong h_0 - k_x^{+1} U_*^{1/\alpha} \ln(x_l/x_0) \quad \text{if } \gamma/\alpha\delta = 1, \tag{4b}$$

with $U_* = (\frac{u}{k} + \varepsilon_0)(\overline{P} - P_0)^{-\beta}$ an external forcing parameter that expresses the balance between tectonic, lithologic and climatic effects, x_0 the length between the drainage divide and the headstream, and h_0 the elevation of the later.

[6] The total relief of a watershed (i.e., the difference between the outlet elevation and the highest peaks of the watershed) is the sum of the fluvial relief, $\Delta h_{fr} = (h_0 - h_r(x_l))$ as defined above, plus the hillslope relief. In active orogens, hillslopes are dominated by landslides [*Hovius et al.*, 1997]: we therefore assume in the following that hillslopes display a critical angle of repose, φ_c, and that they react instantaneously to any local base level drop. We consider that the headstream occurs at the a priori source location (defined by a minimum contributing area), or at the point where the channel slope becomes less than the surrounding hillslope ($S(x_0) < \tan(\varphi_c)$), whichever is lower. For simplicity, a possible transition from hillslope to fluvial channel dominated by debris flows is neglected. The total relief Δh_T expresses:

$$\Delta h_T(x_l) = \Delta h_{fr} + x_0 \tan(\varphi_c). \tag{5}$$

The above classical analysis is useful in describing the main river elevation in a catchment from inception to outlet, but does not provide any analytical value of average watershed height in a given landscape.

3. Geometric Description of a Mountainous Watershed and 1-D Formalism for Mean Elevation

[7] The mean elevation above a point in a river network can be expressed as the volume $V(A_T)$ of the topography above this point divided by its contributing area A_T. This volume can be viewed as the stack of topographic slices, each slice being the density function of elevation in the hypsometric integral. This density strongly depends on channel organisation and branching geometry. If this density function can be expressed as a function of drainage area, then it can be combined with the equilibrium river profile (equations (3)) to provide a topographic volume and the average fluvial relief by integration along the fluvial network:

$$\Delta\overline{h}_{fr}(A_T) = \frac{V(A_T)}{A_T} \cong \frac{1}{A_T}\int_{A_0}^{A_T} f_L(A) S(A) A dA \tag{6}$$

with A_0 the contributing area at the head of the fluvial channel, A_T the area of the studied watershed, and $f_L(A)$ a density function, defined by the length of fluvial network that drains an area A (i.e., $\frac{{}^{fn}L_{[A;A+dA]}}{dA} \xrightarrow[dA\to 0]{} f_L(A)$, with ${}^{fn}L_{[A;A+dA]}$ the total length of fluvial network segments that drain an area comprised between A and $A + dA$). For real networks, despite finite size effects for large drainage areas, this density function roughly follows a power law $f_L(A) = k_L A^{-\omega}$ (Figure 1c). This scaling of the density function can be directly linked to scaling relations in Horton's ordering of a fluvial network (Figure 1), in which a stream segment of order i is related to the following by $\frac{A_{i+1}}{A_i} = R_A$, $\frac{\Delta l_{i+1}}{\Delta l_i} = R_L$, $\frac{n_i}{n_{i+1}} = R_N$, with n_i, Δl_i and A_i the number of stream channels of order i, their average length, and the average contributing area respectively, and where R_A, R_L and R_N are constant and correspond to the area, length and bifurcation ratios. It can be shown that the exponent of the density function can be expressed through the relation $1 - \omega = \frac{Ln(R_L)-Ln(R_N)}{Ln(R_A)}$. The coefficient k_L depends on watershed size (Figure 1c). As long as the drainage density is roughly uniform, k_L is proportional to $\frac{A_T}{\left(A_0^{1-\omega} - A_T^{1-\omega}\right)}$, i.e., to the watershed size A_T when $\omega > 1$ and $A_T \gg A_0$.

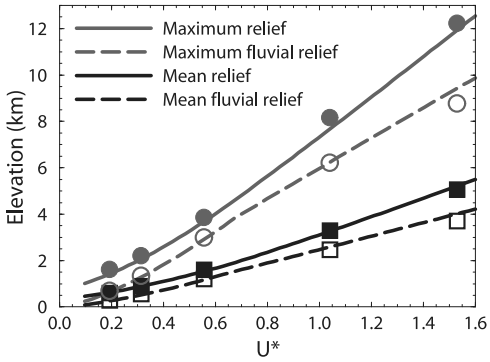

Figure 2. Comparison between the analytic solution (lines) and SPM results (symbols) for different values of the external forcing variable U* applied to the upper Buri watershed. The fluvial incision parameter values are derived from *Lavé and Avouac* [2001]: $\alpha = 0.7$, $\gamma = 0.37$, and the other geometric parameters are $A_S = 0.5$ km^2, $A_T = 3500$ km^2, $k_x = 1.34$ km$^{-0.07}$, $\delta = 0.54$, $k_L = 868$ km$^{1.88}$, $\omega = 1.44$, $\varphi = 40°$. See color version of this figure in the HTML.

[8] Introducing the relation (3a) into equation (6) leads to the following expression for fluvial relief:

$$\Delta\bar{h}_{fr}(A_T) = f_{fr}(A_T, U_*) = \frac{1}{(2-\omega-\gamma/\alpha)}\frac{k_L}{A_T}U_*^{1/\alpha} \cdot \left(A_T^{2-\omega-\gamma/\alpha} - A_0^{2-\omega-\gamma/\alpha}\right) \quad \text{if } \omega+\gamma/\alpha \neq 2 \qquad (7a)$$

and

$$\Delta\bar{h}_{fr}(A_T) = \frac{k_L}{A_T}U_*^{1/\alpha} Ln(A_T/A_0) \qquad \text{if } \omega+\gamma/\alpha = 2 \qquad (7b)$$

[9] The mean topographic elevation of a watershed reflects the sum of this mean fluvial relief and the hillslope component. In theory, the average hillslope relief could be computed following the same approach as above by integration of the critical slope $S = \tan(\varphi_c)$ up to the crests as long as $\omega \leq 2$. However, the power law behaviour of the length density function breaks at the hillslope/channel transition (Figure 1c) and thus prohibits simple integration of equation (6). Another approach considers that the average distance, d_0, between the crests and the fluvial network is roughly equal to the drainage area divided by 2 times the cumulated length of channel network in this basin, i.e., ${}^{fn}L_{[A_0;A_T]} \cong \int_{A_0}^{A_T} f_L(A)\mathrm{d}A$. The average hillslope relief thus corresponds to $\Delta\bar{h}_{hs} = {}^{d_0}/_2 \tan(\varphi_c) = {}^{A_T}/_{4^{fn}L_{[A_0;A_T]}} \tan(\varphi_c)$. Nevertheless, this formulation is valid as long as the fluvial network is not too steep and the meander wavelengths are larger than the hillslope dimension. Here, the studied cases require an empirical adjustment of d_0 by a factor $\sim$1.3.

[10] Equation (7) is valid as long as the length density function does not depend on uplift rate. It has been shown, however, that the scaling relations in fluvial networks, in particular the Horton's organization, are not very sensitive to the geometry of the network [*Kirchner*, 1993], and do not depend significantly on uplift rates [*Hurtrez et al.*, 1999]. To test this, we computed the synthetic topography from the upper Buri river network (shaded area in Figure 1)) using a classic 2-D SPM [e.g., *Beaumont et al.*, 1992] with the same parameters and erosion laws, i.e., a detachment-limited model for mountain river incision, and hillslope erosion governed by landsliding through a critical angle of stability. For different values of the external forcing parameter U_*, the analytic solution and SPM results display very consistent results and dependency to U_*, both for the fluvial relief and the whole topography (Figure 2). This supports our initial hypothesis that river network geometry, scaling characteristics and, to a lesser extent, the empirical correction factor for the hillslope relief calculation are relatively insensitive to the uplift rates.

4. Application of the 1-D Model to a Cylindrical Range

4.1. Cross-Range Profiles at Steady State

[11] Although real river networks or those produced in SPMs are relatively insensitive to uplift rate, they can be strongly influenced by the spatial uplift patterns. In many mountain ranges, the river network tends to be oriented perpendicular to the uplifting structure or range axis. Such drainages are characterized by regular outlet spacing [*Hovius*, 1996], and parallel rectangular basins. Each basin comprises a major linear river perpendicular to the mountain axis, characterized by Hack's exponent δ closer to 1 than to 0.5, and a series of tributaries feeding the major river, characterized by a more dendritic channel network. To fully compute the topography of such settings, relation (4) is used to describe the profile of the major rivers, i.e., of the local base level for the tributaries, whereas equation (7) yields the fluvial relief associated with these tributaries.

[12] To test this approach both in terms of steady state mountain profiles and of transitory response, a synthetic, symmetric low elevation topography was created with 6 roughly similar watersheds (Figure 3b). The different relationships and scaling characteristics of these basins were first computed (see details in Text S2 and Figure S1 in the auxiliary material) and introduced into relations (4) and (7) in order to compute the minimum, mean and maximum elevation of the cross range profile at steady state. Following the approach above, the SPM was used to compute the corresponding profiles, and, as observed for the upper Buri watershed, provides results consistent with the 1-D solution (Figure 3).

4.2. Transient Response During Waxing Phase: An Inverse Method to Generate and Erode a 1-D Topography

[13] In the above example, the landscape initially presents a nearly flat undulated topography close to the base level elevation. In response to the tectonic uplift (fixed at 2 mm/yr), an intense backward wave of erosion propagates along the main stream and its tributaries. From the uplift initiation to steady state attainment, the landscape is thus characterized by a transient response. Whereas equation (7) applies only to steady state regimes, we speculate that it could provide a satisfying first order approximation to the relationship between average elevation of the tributary watershed and denudation rate provided the geomorphic system is not too far from the equilibrium. To test this, we

consider the average denudation in a watershed, which can be computed from inverting equation (7a):

$$E* \approx f_{fr}^{-1}\left(\Delta\overline{h}_{fr} = \overline{h} - d_0/2\tan(\varphi_c) - h_R\right) = \left(\frac{(2-\omega-\gamma/\alpha)A_T}{k_L}\frac{\Delta\overline{h}_{fr}}{\left(A_T^{2-\omega-\gamma/\alpha} - A_0^{2-\omega-\gamma/\alpha}\right)}\right)^{\alpha} \quad (8)$$

with $\overline{h}$ the mean elevation of the lateral tributary watershed, h_R the elevation of the confluence of this tributary with the cross-range river, $E* = (\frac{e}{k} + \varepsilon_0)\,(P - P_0)^{-\beta}$ and e the average erosion rate in the tributary basin. Practically, because d_0 depends on the erosion rate, the inversion has to be performed iteratively. The steady state is similarly attained in both approaches after ~1.5 Myr (Figure 4). More importantly, the minimum, maximum and average elevation cross-range profiles at the different time steps (Figure 4a) and the mean denudation curves (Figure 4b) are remarkably consistent: the relative difference between the two denudation curves lies between 0 and 25%, and the difference in terms of topographic profiles is still less pronounced. The 1-D model tends, however, to slightly overestimate the denudation rates in the first half of the transient response.

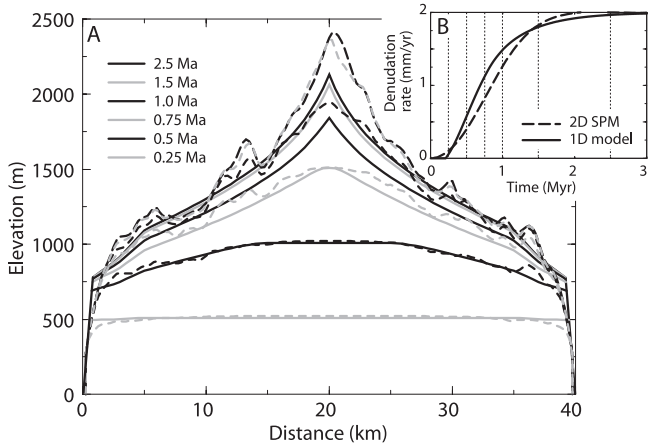

Figure 4. Comparison between the 1-D model (solid lines) and SPM (dashed lines) during the waxing phase of the mountain range of Figure 3b. (a) Cross-range profiles at different time steps. (b) Evolution of the landscape denudation rate.

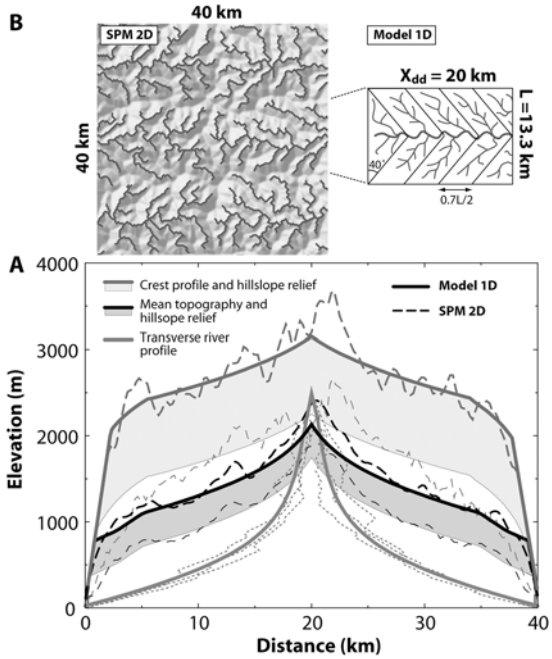

Figure 3. (a) Comparison between the cross-range steady state profiles predicted by the 1-D model (solid lines) and SPM (dashed lines) for a synthetic cylindrical mountain range (b) in terms of mean topography and fluvial landscape profiles, river and ridge profiles. In the 1-D analysis, the evolution of the main river in each transverse rectangular watershed is controlled by equation (2) but replacing x_l by $X = x_l/\sigma$, with X the cross range abscissa taken from the drainage divide and σ the average sinuosity of this main stem (here $\sigma = 1.43$). Above their confluence with the main stem, the parallelogram shape tributaries are governed by equation (7), with $A_S = 0.5$ km^2, $A_T = 31$ km^2, $k_x = 1.55$ km$^{-0.07}$, $\delta = 0.54$, $k_L = 6.5$ km$^{1.3}\omega = 1.15$, $\varphi = 40°$. The fluvial incision parameter values are similar to previous test of Figure 2, and $U* = 0.55$, $\beta = 0.33$, $(P\text{-}P_s) = 1.45$ m/yr, $k = 3.65$. See color version of this figure in the HTML.

5. Discussion

[14] In the above analytic approach, the mean elevation of a watershed at steady state (equation 7) and the profile of its longest stream (equation 4) are governed by the same dependency to fluvial incision law and external forcing parameters. It thus provides a more physical framework to the approaches that try to link denudation with relief, mean elevation, lithology, and/or climate. It particularly shows that deriving a general relation from various watersheds in which uplift rate, lithology or precipitation are not uniform can lead to substantial scatter.

[15] In theory, the results are restricted to river networks driven by detachment-limited incision. However, for river profiles at steady state, equation (3a) has also been found to be consistent with incision laws other than detachment-limited cases, that explicitly include the role of sediment supply (transport limited…) [*Whipple and Tucker*, 2002]. Consequently, the proposed analytical solution (7) is directly applicable to any incision law that can be cast as a power function of slope and drainage area. The method, however, is invalid for low uplift rates because of the increasing role of the chemical erosion and dependence of the hillslope angle to the uplift rate.

[16] Our final synthetic example also suggests that the 1-D analysis provides a reasonable method to describe the transient response of a growing mountain range. Its direct application to describe topographic evolution of a mountain range during its waning phase could be limited, however, by an eventual shift of geomorphic systems from detachment-limited to transport-limited conditions [*Whipple and Tucker*, 2002], which would require a concomitant shift of the erosion parameters. In any case, this new approach offers potential improvements for computing erosion and mean surface elevation in numerical models. In the 2-D case, it

helps both to dissociate the fluvial incision along cross-range rivers from the topographic denudation, and to compute minimum, maximum and mean topography. For 3-D models, where 2-D SPM are required to model erosion and topography, this formalism may help to improve the spatial resolution. For example, a large scale deformable mesh, where the cell size is much larger than the hillslope length, could account for the evolution of the fluvial network in terms of highest order streams, whereas the proposed analytic solution describes tributary response and hillslope relief between the distant mesh nodes.

References

Beaumont, C., P. Fullsack, and J. Hamilton (1992), Erosional control of active compressional orogens, in *Thrust Tectonics*, edited by K. R. McClay, pp. 1–18, Chapman and Hall, New York.

Godard, V., R. Cattin, and J. Lavé (2004), Numerical modeling of mountain building: Interplay between erosion law and crustal rheology, *Geophys. Res. Lett.*, *31*, L23607, doi:10.1029/2004GL021006.

Hovius, N. (1996), Regular spacing of drainage outlets from linear mountain belts, *Basin Res.*, *8*, 29–44.

Hovius, N., C. P. Stark, and P. A. Allen (1997), Sediment flux from a mountain belt derived by landslide mapping, *Geology*, *25*, 231–234.

Hurtrez, J. E., F. Lucazeau, J. Lavé, and J. P. Avouac (1999), Investigation of the relationships between basin morphology, tectonic uplift and denudation from the study of an active fold belt in the Siwaliks Hills (central Nepal), *J. Geophys. Res.*, *104*, 12,779–12,797.

Lavé, J., and J. P. Avouac (2001), Fluvial incision and tectonic uplift across the Himalayas of central Nepal, *J. Geophys. Res.*, *106*, 26,561–26,592.

Kirchner, J. W. (1993), Statistical inevitability of Horton's laws and the apparent randomness of stream channel networks, *Geology*, *21*, 591–594.

Pinet, P., and M. Souriau (1988), Continental erosion and large-scale relief, *Tectonics*, *7*, 563–582.

Whipple, K. X., and G. E. Tucker (1999), Dynamics of the stream-power river incision model: Implications for height limits of mountain ranges, landscape response timescales, and research needs, *J. Geophys. Res.*, *104*, 17,661–17,674.

Whipple, K. X., and G. E. Tucker (2002), Implications of sediment-flux-dependent river incision models for landscape evolution, *J. Geophys. Res.*, *107*(B2), 2039, doi:10.1029/2000JB000044.

J. Lavé, Laboratoire de Géodynamique des Chaînes Alpines, BP53, F-38041 Grenoble, France. (jlave@ujf-grenoble.fr)